

ReSIM: Re-ranking Binary Similarity Embeddings to Improve Function Search Performance

Gianluca Capozzi¹, Anna Paola Giancaspro², Fabio Petroni³, Leonardo Querzoni², and Giuseppe Antonio Di Luna²

¹KASTEL Security Research Labs, Karlsruhe Institute of Technology, gianluca.capozzi@kit.edu

²DIAG, Sapienza University of Rome, Italy, {giancaspro,querzoni,diluna}@diag.uniroma1.it

³European Molecular Biology Laboratory (EMBL) Rome, Italy, fabio.petroni@embl.it

Abstract

Binary Function Similarity (BFS), the problem of determining whether two binary functions originate from the same source code, has been extensively studied in recent research across security, software engineering, and machine learning communities. This interest arises from its central role in developing vulnerability detection systems, copyright infringement analysis, and malware phylogeny tools. Nearly all binary function similarity systems embed assembly functions into real-valued vectors, where similar functions map to points that lie close to each other in the metric space. These embeddings enable function search: a query function is embedded and compared against a database of candidate embeddings to retrieve the most similar matches.

Despite their effectiveness, such systems rely on bi-encoder architectures that embed functions independently, limiting their ability to capture cross-function relationships and similarities. To address this limitation, we introduce ReSIM, a novel and enhanced function search system that complements embedding-based search with a neural re-ranker. Unlike traditional embedding models, our reranking module jointly processes query-candidate pairs to compute ranking scores based on their mutual representation, allowing for more accurate similarity assessment. By re-ranking the top results from embedding-based retrieval, ReSIM leverages fine-grained relation information that bi-encoders cannot capture.

We evaluate ReSIM across seven embedding models on two benchmark datasets, demonstrating consistent improvements in search effectiveness, with average gains of 21.7% in terms of nDCG and 27.8% in terms of Recall.

1 Introduction

In recent years, research on Binary Function Similarity (BFS) has flourished [2, 8, 24, 30–32, 43, 52, 56]. The BFS problem consists of assigning a similarity score to two binary functions that is maximized when the functions originate from the same source code (even if compiled with different compilers or optimization levels) and minimized when they are unrelated.

Most state-of-the-art approaches address BFS through embedding-based architectures [2, 43, 52]. Specifically, a Deep Neural Network (DNN) encodes each function into a fixed-dimensional vector (i.e., the embedding) intended to capture its semantics, and the similarity between two embedded functions is efficiently computed in the embedding space (e.g., using cosine similarity or another distance metric), with higher values assigned to functions stemming from the same source code. This approach is known in information retrieval as the bi-encoder paradigm [21, 47] and enables scalable function search. Specifically, given a large pool of functions (e.g., functions affected by known CVEs), their embeddings can be precomputed, indexed, and queried efficiently through maximum inner product search (MIPS), typically implemented via matrix multiplication, to return the top- k most similar functions

to a certain query. In the case of a vulnerability detection system, the retrieved functions correspond to those most likely to contain the same vulnerability as the query function. Embedding-based function search has therefore become the de facto evaluation protocol for BFS systems [2, 52] and underpins a broad range of security applications, including code clone detection, vulnerability detection, copyright infringement analysis, malware analysis and phylogeny, and reverse engineering support.

However, this approach presents a significant limitation. Bi-encoders compute embeddings for the query and each candidate independently, which prevents the model from learning cross-function relationships. In practice, the embedding must condense all potentially relevant information, without knowing which embeddings it will later be compared against. This is particularly limiting in the function search scenario, where the top-ranked results may appear very similar at the binary level (e.g., due to compiler artifacts, common library usages) but originate from different source code. As a result, embedding models may retrieve plausible candidates yet misorder them at the very top positions, degrading retrieval metrics.

In this paper, we address this gap by introducing a re-ranking approach to complement embedding-based

function search. First, an embedding model efficiently retrieves the top- w candidates; then, a neural re-ranker reorders these candidates using a joint query-candidate representation to model cross-function interactions and returns the top- k results.

The inspiration for using a re-ranker comes from the information retrieval literature. The field of information retrieval has long employed multi-stage architectures to balance efficiency and accuracy [39, 53]. In the first phase, a recall-oriented candidate retrieval model efficiently identifies potentially relevant items from a large corpus. Modern systems leverage bi-encoder models that independently encode queries and documents into dense vectors. These embeddings enable efficient similarity search via MIPS, but sacrifice fine-grained semantic interactions since queries and documents interact only through vector similarity. In the second phase, a precision-oriented re-ranking model refines these candidates using more sophisticated scoring. This phase employs cross-encoder architectures that jointly process query-document pairs, enabling deeper semantic interactions [26, 37]. While computationally expensive, cross-encoders improve retrieval performance and have become standard in Retrieval-Augmented Generation (RAG) systems [22, 44].

In this paper, we propose **ReSIM**, a novel two-stage function search pipeline that leverages a cross-encoder re-ranking model to augment embedding-based function search. First, an embedding-based system efficiently retrieves via MIPS the top- w candidates from an indexed database; then, a re-ranker jointly processes the query-candidate pairs to re-rank these w functions and return the top- k results, with $k \leq w$. Importantly, ReSIM is agnostic to the underlying embedding model.

Experiments show that ReSIM significantly improves the nDCG @ k (normalized Discounted Cumulative Gain, a standard metric for search engines [19, 38]) and the Recall @ k of the considered embedding models.

1.1 Contributions

This paper proposes the following contributions:

- We train and publicly release the ReSIM pipeline for x86-64 assembly functions. Our re-ranker is based on the **DeepSeek-R1-Qwen3-8B** [13] model.
- We evaluate ReSIM by constructing several function search systems, each using a different BFS embedding model. Specifically, we consider seven embedding models (Gemini [56], SAFE [32], jTrans [52], CLAP [51], BinBERT [2], Trex [43], and PalmTree [23]) chosen for their strong performance and their diversity in terms of DNN architectures and training methodologies.
- We demonstrate that, for $k \in \{5, 10, 15, 20, 25, 30\}$ and across two datasets, ReSIM consistently improves all evaluated systems (average Recall from 0.59 to 0.72; average nDCG from 0.69 to 0.82). Moreover, we analyze the impact of the window size w on the computational efficiency and the performance of ReSIM.

- We show that ReSIM is able to ensemble different embedding models, leading to a further 3% Recall increase on a dataset composed of several toolchains.
- We show that there is an important transfer of knowledge from the pre-training of **DeepSeek-R1-Qwen3-8B** [13], even if it was not tailored on assembly language.
- We evaluate ReSIM on the vulnerability detection task, considering a large benchmark of CVEs.
- We release our fine-tuning and evaluation code at <https://github.com/Sap4Sec/reSIM.git>

2 Background

This section provides a general overview of the key concepts of embedding-based binary function similarity.

2.1 Embedding-based Function Search

Binary Function Similarity (BFS) consists of checking whether two binary functions have been compiled from the same source code [32]. If this condition holds, the two functions are considered to be *semantically similar*. A *BFS embedding model* is a deep neural network (DNN) ϕ that takes as input an assembly function f and returns a vector $\vec{f} \in \mathbb{R}^n$. Given two functions f_1 and f_2 with embeddings $\vec{f}_1 = \phi(f_1)$ and $\vec{f}_2 = \phi(f_2)$, their similarity score is measured via cosine similarity $sim = \cos(\vec{f}_1, \vec{f}_2)$. This process is visible in Figure 1. Ideally, sim should be 1 when f_1 and f_2 originate from the same source code, although they may have been compiled with different compilers/optimization levels, and 0 otherwise.

Within this context, the **function search** problem aims to identify the top- k functions within a pool that are most similar to a given query. Formally, given a query function f_q , a pool of binary functions P , and a set $V \subseteq P$ of variants of f_q (i.e., functions semantically equivalent to f_q), we denote by $\text{top-}k(f_q, P)$ the set of top- k functions returned by the search (ranked by similarity).

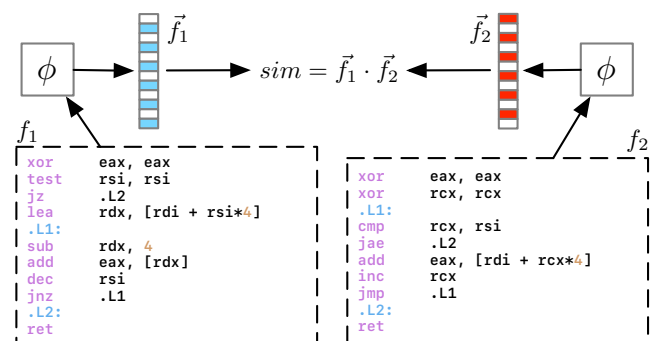


Figure 1: Embedding-based BFS pipeline. The functions f_1 and f_2 are processed in isolation by the BFS model ϕ to produce their embedding representations \vec{f}_1 and \vec{f}_2 , which are then compared using cosine similarity to get the final score.

In a perfect function search system, every element of V appears in the first $|V|$ positions of $\text{top-}k(f_q, P)$. That is, an effective function search system maximizes the overlap $|V \cap \text{top-}k(f_q, P)|$. Note that this is only possible when $k \geq |V|$; when $k < |V|$, the requirement is infeasible. In any case, even when $k < |V|$, we can evaluate system performance with standard retrieval metrics. The Recall at rank k is defined as:

$$\text{Recall}@k(f_q) = \frac{|V \cap \text{top-}k(f_q, P)|}{|V|}, \quad (1)$$

and the normalized discounted cumulative gain at rank k (nDCG@ k) defined on the ordered list of top- k retrieved results $[f_1, f_2, \dots, f_k]$ as:

$$\text{nDCG}@k(f_q) = \frac{\sum_{i=1}^k \frac{S(f_i, f_q)}{\log(1+i)}}{\sum_{i=1}^{\min(k, |V|)} \frac{1}{\log(1+i)}}. \quad (2)$$

Here, $S(f_i, f_q)$ is an indicator function equal to 1 if f_i is similar to the query function f_q , and 0 otherwise. The denominator corresponds to the score of a perfect ranking, while the numerator represents the score achieved by the system under evaluation. The nDCG ranges between 0 and 1, and accounts for the ordering of items in the top- k results, rewarding rankings in which relevant items appear earlier.

As an example, consider two result lists for the same query: (s, s, d, d) and (d, d, s, s) , where s indicates that the corresponding position is occupied by a similar function and d otherwise. Although these two results have the same Recall, nDCG assigns a higher score to the first ranking, since the relevant items appear in earlier positions.

BFS embedding systems can be adapted to the function search task. Concretely, this is done by transforming the pool P into a set of vectors by applying ϕ to each function in P , thus obtaining \mathcal{P} . Given a query function f_q , its embedding $\vec{f}_q = \phi(f_q)$ is computed and multiplied by each vector in \mathcal{P} , obtaining a similarity score between f_q and each function in P . The corresponding functions in P are then ranked according to the aforementioned similarity scores, and the top- k results are returned. Since the vectorization of the pool needs to be computed only once, while the query lookup can be efficiently performed using matrix multiplication followed by sorting, this system design is scalable.

2.2 BFS Embedding Models

BFS embedding models can be classified according to three important dimensions:

1. **DNN architecture.** Early work mainly relied on Graph Neural Networks (GNN) [24, 56], and Recurrent Neural Networks (RNN) [32]. More recent approaches adopt transformer-based architectures [2, 43, 51, 52], to better capture long-range dependencies and handle long instruction sequences.
2. **Function representation strategy.** Another important difference is the way they represent assembly functions. GNN-based methods typically

operate on representations derived from the Control Flow Graph (CFG). In some cases [24, 56], nodes (i.e., the basic blocks of the CFG) are represented as vectors of manual features (e.g., the number of mathematical operations, the number of strings referenced, ...). Sequence-based models (i.e., RNN and transformers) consume assembly instruction sequences produced by linear disassembly [32, 52], or execution traces [2, 43]; these instructions are typically preprocessed and normalized to mitigate the out-of-vocabulary (OOV) problem.

3. **Training.** GNN/RNN-based approaches are commonly trained using a Siamese architecture [3, 32, 47]. This technique consists of using multiple embedding networks, each producing the embedding of a function, which are then jointly trained by minimizing a loss function (typically, in the form of contrastive or triplet loss). Transformers are typically pre-trained with self-supervised objectives specific to assembly code (e.g., *jump target prediction* [52], *execution language modeling* [2]), then fine-tuned for function similarity on pairs or triplets.

These axes have guided our choice of the embedding models to use in our tests, as we will describe in Section 3.2.

3 ReSIM: Re-ranked Function Search

Our contribution is **ReSIM**, a two-stage pipeline that enriches the embedding-based function search system described in Section 2.1 by integrating a re-ranking neural network. A re-ranker is a function ρ that takes as input two assembly functions, f_1 and f_2 , and outputs a ranking score $\rho(f_1, f_2) \in [0, 1]$, where values close to 1 indicate that the two functions are similar, and values close to 0 indicate dissimilarity.

Figure 2 illustrates the overall architecture of **ReSIM**. This is based on a BFS embedding model ϕ and a re-ranker ρ . A query function f_q is transformed into an embedding vector $\vec{f}_q = \phi(f_q)$. The embedding vector is compared with the embedded pool \mathcal{P} using cosine similarity to obtain a set W of the most similar functions, referred to as the *window set*, of size w . For each pair (f_q, f_i) with $f_i \in W$, the value $\rho(f_q, f_i)$ is computed, yielding an ordered list of rankings $[r_1, r_2, \dots]$. This ranking is used to extract a set of k functions from W , which are the top- k results of our function search system.

As an example, let us consider a query f_q with $|V| = 4$. Assume that the embedding-based function search produces a window $W = [s, d, s, d, s, s]$ of size 6, where s represents a function similar to the query and d a dissimilar one. In this case, the Recall@4 is 2/4, and the nDCG@4 is 0.59. After applying the re-ranking, we obtain $W' = [s, s, s, d, s, d]$, with a Recall@4 of 3/4 and an nDCG@4 of 0.83.

We stress that the proposed system is general enough that any embedding model ϕ can be used. In our exper-

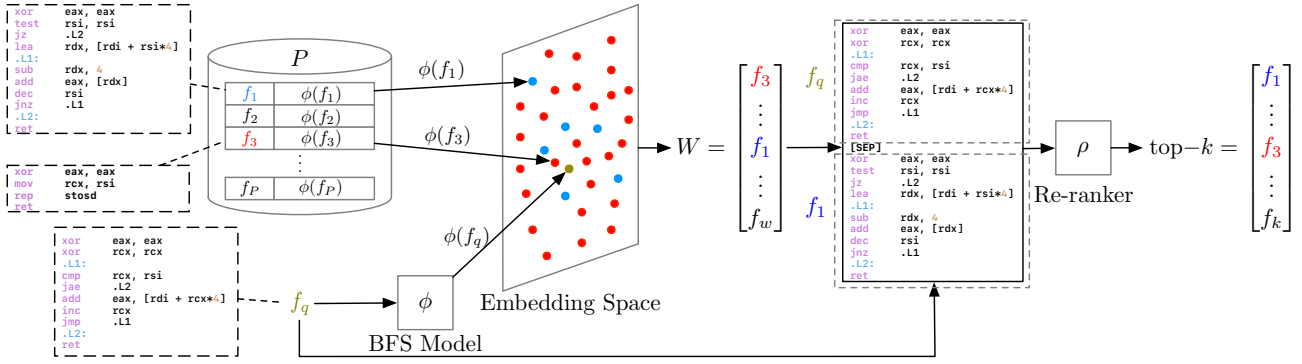


Figure 2: ReSIM pipeline. (i) The BFS bi-encoder ϕ maps the query function f_q to an embedding $\phi(f_q)$. (ii) A similarity measure $sim(\phi(f_q), \phi(f))$ is evaluated against the embeddings of all the functions $f \in P$, and the window set W containing the top- w candidates is retrieved; blue dots denote embeddings of functions semantically similar to the query, whereas red dots denote dissimilar ones. (iii) Each $f \in W$ is paired with the query and scored by the re-ranker cross-encoder $\rho(f_q, f) \in [0, 1]$, which reorders W to produce the final top- k list.

imental evaluation, we will test seven different models, and there are no requirements for using a specific combination of ϕ and ρ .

Relationship between W , P , and k

There is a subtle effect determined by the relationship among the size of the window W , the size of the pool P , and the value of k . If $|P| = |W|$, the embedding model ϕ becomes irrelevant, and the performance is determined solely by ρ . This occurs because all the functions in the pool are ordered by ρ , and the final ranking is precisely the one from which the top- k functions are selected. Conversely, when $|W| = k$, the order produced by ρ does not influence the functions inside the top- k , and therefore cannot improve the system’s recall at k , although it may still affect other metrics such as nDCG.

This relationship also impacts the total running time of a query lookup. When $|W| = |P|$, the re-ranker ρ must be executed once for each function in P . Neglecting possible parallelization and assuming an average runtime $T(\rho)$ for ρ , the running time of the re-ranking phase is $|P|T(\rho)$. When $|W| = k$, the running time is $kT(\rho)$, meaning that execution time decreases as $|W|$ decreases. However, the relationship between the $|W|$, the Recall and nDCG is not straightforward.

It is possible that the embedding model ϕ and the re-ranker ρ analyze different aspects of assembly functions. For instance, ϕ might leverage execution-related information to produce its embeddings, while ρ relies solely on static features. Therefore, it is not clear whether applying ρ to the entire dataset P would yield better performance than applying it only to the window W . It could be that ϕ acts as an effective pre-filter, removing certain false positives that ρ would be unable to, thereby providing ρ with a refined window W that ultimately boosts the system’s performance. Therefore, the impact of the window size on these outcomes will be analyzed in our experimental evaluation.

Ensembling embedding models

The basic re-ranking architecture can be extended to use an ensemble of embedding models, ϕ_1, \dots, ϕ_t . Using the query, we retrieve several candidate windows W_1, \dots, W_t , where each W_i is obtained from the model ϕ_i . Each candidate window W_i is first re-ranked individually using ρ , producing a set of re-ranked lists W'_1, \dots, W'_t . Each function in these lists now has an associated re-ranker score. The final result is constructed by merging all lists and removing duplicates. The final, de-duplicated list is then sorted by these scores to produce the top- k results. The main motivation for using an ensemble of embedding models is to exploit their diversity (see Section 2.2), under the assumption that different models may perform better on different binary functions. From our experiments we observe that embedding models fare better on dataset generated with toolchains used during training or fine-tuning. It is important to note that the similarity scores produced by different embedding models are *not directly comparable*. The embedding model ϕ_X might yield an average similarity of 0.8 to similar pairs, while a model ϕ_Z may assign an average similarity of 0.9 to similar pair (see [4]). Because of these differences in scale and calibration across models, one cannot simply aggregate raw similarity scores to construct an ensemble, the re-ranking score avoid this problem.

3.1 Re-ranker Architecture

Following the approach in [37], we instantiate ρ as a transformer-based **cross-encoder** fine-tuned for binary pairwise ranking. Starting from a pretrained model, we attach a task-specific classification head and fine-tune the model end-to-end. For encoder-only (BERT-like [50]) models, the head operates on the hidden state of the first token; for causal decoder-only models (i.e., Llama [12], Qwen [58]), it uses the hidden state of the last non-padding token. The classification head outputs a single logit, which is used as a ranking score.

Figure 3 illustrates the re-ranking process. The re-ranker model is provided with the preprocessed lin-

ear disassembly of the two functions being compared. Specifically, given a query function f_q and a candidate $f_i \in P$, we concatenate the two sequences with a special separator (e.g., f_q [SEP] f_i) to form a single input sequence.

3.1.1 The DeepSeek-R1-Qwen3-8B Model

In what follows, we focus on the **DeepSeek-R1-Qwen3-8B** [13] as it is the re-ranker architecture we employ for our tests. This is an 8B-parameter dense transformer obtained distilling the reasoning of DeepSeek-R1 into Qwen3-8B [58].

DeepSeek-R1 itself is produced via post-training that combines supervised fine-tuning and reinforcement learning to strengthen reasoning capabilities; DeepSeek-R1-Qwen3-8B inherits these behaviors through distillation into Qwen3-8B. We refer readers to [13] for details of the training pipeline.

3.1.2 Instructions Preprocessing and Tokenization

To reduce variability and mitigate the OOV problem, we preprocess and normalize the two functions under analysis. We first rebase addresses in the assembly code, then we apply the following normalization steps:

- Immediate values, memory addresses, and offsets greater than a fixed threshold (5,000) are replaced with the special token **IMM**.
- Jump targets within the function address space are replaced with a relative offset.
- User-defined function names are replaced with the special token **func**.
- For calls to **libc** functions, the target address is replaced with the function name.

After concatenating the two normalized sequences using the special token [SEP], we finally tokenize the resulting sequence using architecture-specific strategies tailored to the re-ranker model (further details are in Section 4.3).

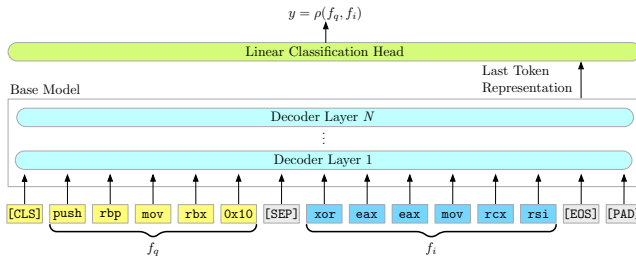


Figure 3: Re-ranking pipeline with a decoder-only transformer ρ (cross-encoder). The two input functions f_q and f_i are tokenized and concatenated with a [SEP] token to form a single sequence processed by the N -layer decoder. A classification head reads the hidden state of the last non-padding token and outputs a logit y , which is then used to score and re-rank the candidates in W .

3.1.3 Re-ranker Finetuning

We fine-tune DeepSeek-R1-Qwen3-8B on the binary pairwise ranking objective: given two binary functions f_1 and f_2 , the model predicts a ranking score $y \in \mathbb{R}$, with higher values assigned to functions compiled from the same source code.

To enhance the re-ranker decision boundaries, we incorporate hard negatives during fine-tuning. In particular, different embedding models capture complementary aspects of binary code, so sampling hard negatives from three distinct models allows us to introduce different knowledge aspects into our re-ranker model. Thus, for each anchor f_a , we construct: a positive (f_a, f^+) pair, where f^+ is a function semantically equivalent to f_a (i.e., compiled from the same source code [32]), and three hard negative pairs (f_a, f_i^-) , with $i \in \{1, 2, 3\}$, where each f_i^- is sampled from the top- k most similar functions that are not semantically equivalent to f_a , according to the BinBERT [2], jTrans [52], and CLAP [51] models.

For each triplet (f_a, f^+, f_i^-) , we separately compute $y^+ = \rho(f_a, f^+)$ and $y_i^- = \rho(f_a, f_i^-)$, and then we optimize the margin ranking loss $\mathcal{L}(y^+, y_i^-, m) = \max(0, -(y^+ - y_i^-) + m)$, where m is the margin hyperparameter. Intuitively, the loss enforces the positive ranking y^+ to exceed the negative one y_i^- by at least m , forcing a clear separation between positive and hard negative pairs in the score space.

To reduce trainable parameters and enable efficient fine-tuning of the 8B cross-encoder, we adopt LoRA [16], combining it with 4-bit QLoRA quantization [57]. LoRA applies adapters at different projections (i.e., attention-level, MLP) of the base model; each adapter decomposes the corresponding projection matrix into two low-rank adaptations whose output is scaled and added to the frozen projection output. During fine-tuning, only the adapter weights and the classification head are updated while the base model remain fixed. At inference time, the adapter update can be merged into the base weights. Further details about LoRA hyperparameters and target projections are in Section 4.3.

3.2 BFS Embedding Models

We evaluate ReSIM on seven BFS embedding models that span the main design choices discussed in Section 2.2 (architecture, function representation, and training). This diversity helps us assess whether re-ranking is consistently beneficial across heterogeneous encoders.

The **Gemini** model [56] uses a Siamese graph neural network (Structure2Vec [6]) over Attributed CFGs, producing function embeddings by aggregating node representations.

The **SAFE** model [32] embeds linear disassembly with a recurrent architecture trained in a Siamese setup; it builds instruction embeddings (word2vec-inspired [33]) and aggregates them with self-attention to obtain a function vector.

The **jTrans** model [52] adapts BERT to assembly by tokenizing mnemonics and operands and handling jump targets explicitly; it is pretrained with assembly-specific objectives (masked language modeling and jump-target prediction) and then fine-tuned for similarity with a contrastive loss.

The **CLAP** model [51] learns assembly embeddings under natural-language supervision by aligning a jump-aware RoBERTa-like encoder [28] with a text encoder [18] using contrastive learning (InfoNCE [41]); at inference time, it embeds functions from assembly alone.

The **BinBERT** model [2] is an encoder-only transformer pretrained to be execution-aware by leveraging symbolic-execution information alongside assembly; it is then fine-tuned for BFS in a Siamese/triplet setting.

The **PalmTree** model [23] is an assembly transformer pretrained with self-supervised objectives on normalized disassembly (e.g., masking and context prediction). Because it outputs instruction-level embeddings, we follow prior work [2] and aggregate instructions (via an LSTM) to obtain function-level vectors.

The **Trex** model [43] leverages transfer learning with a hierarchical transformer [42] pretrained on execution traces; for function search it produces embeddings from linear disassembly by pooling final-layer representations and applying a small feed-forward projection.

4 Datasets and Implementation Details

In this section, we describe the datasets used for our experimental evaluation and the implementation details.

4.1 Fine-tuning Dataset

To fine-tune our re-ranker, we use a subset of the BinCorp-26M dataset from [52]. According to the authors, this dataset contains 26M functions extracted from 48,130 binaries selected from the official Arch-Linux packages and Arch User Repository, compiled for the x86-64 architecture using the gcc compiler with optimization levels ranging from $-O0$ to $-Os$. Specifically, we construct a contrastive fine-tuning corpus from the Train split of BinCorp-26M. Following the approach detailed in Section 3.1.3, we select 833,739 anchor functions and, for each anchor f_a , we create three triplets (f_a, f^+, f^-) , where each anchor has been paired with a random positive sample and three hard negatives. This process yields a total of 2,651,217 triplets.

4.2 Evaluation Datasets

To precisely identify the performance increase attributable to the re-ranker while avoiding confounding factors, we use several distinct datasets for testing. Specifically, we use:

BinCorp Dataset. From the Test split of BinCorp-26M [52], we select 5,000 query functions. For each query, we consider its set of five semantically similar

functions present in the corpus (including the query itself), yielding an evaluation pool of 25,000 functions (see Section 4.1 for further details).

MultiComp Dataset. This benchmark is a subset of SimTestData [2], obtained by compiling for the x86-64 architecture the following open-source projects: putty0.74, ImageMagick-7.0.10-62, sqlite-3.34.0, gmp-6.2.0, zlib1.2.11, nmap-7.80, and libtomcrypt-1.18.2. In contrast to BinCorp, MultiComp exhibits greater heterogeneity: binaries are produced with multiple versions of gcc (versions 5, 7, and 9), clang (versions 3.8, 6.9, and 9), and icc (version 21), using optimization levels ranging from $-O0$ to $-O3$. We select 1,000 queries among the available 5,000, yielding a pool of 11,622 functions. On average, each query has 11.7 similar in the pool.

4.3 Implementation Details

We implement our re-ranker in Python using the HuggingFace library version 4.57.1. Specifically, for our evaluation, we consider the DEEP re-ranking architecture, finetuned from DeepSeek-R1-Qwen3-8B¹ [13] following the procedure described in Section 3.1.3. Specifically, we fine-tuned this model following the QLoRA approach [57], which combines 4-bit quantization with LoRA [16]. Specifically, we set rank $r = 16$, scaling $\alpha = 16$, and dropout $p = 0.05$, targeting the attention (q, k, v, o) and MLP projections (gate, up, down) while keeping biases frozen and initializing LoRA weights.

Furthermore, we fine-tuned DEEP for one epoch with a learning rate of 1×10^{-4} , a maximum input length of 2,048 tokens, and a per-device batch size of 8. After preprocessing (see Section 3.1.2), we employed left-side tokenization (left truncation), prioritizing the tail of each input function. This is motivated by previous observations that many embedding-based models disproportionately focus on function prologues [5, 54].

For all embedding models, we use the authors’ official implementations and publicly released checkpoints, without additional retraining, except for Gemini, for which no official implementation is available.

Finally, we disassemble binaries from the BinCorp and MultiComp codebases with Ghidra². The only exceptions are the jTrans and CLAP evaluations on BinCorp, where we used the IDA³ disassembly and scripts supplied with those cases (as required by the original setups).

5 Experimental Evaluation

Our evaluation comprises the following research questions:

¹<https://huggingface.co/deepseek-ai/DeepSeek-R1-0528-Qwen3-8B>

²<https://github.com/NationalSecurityAgency/ghidra>

³<https://hex-rays.com/>

Table 1: nDCG and Recall for the considered BFS models using DEEP as reranker ($w = 200$, $k \in \{5, 10, 15, 20, 25, 30\}$), evaluated on pools from BinCorp and MultiComp. Best performances per dataset shown in **bold**.

Dataset	BFS model	re-ranker	nDCG					Recall						
			@5	@10	@15	@20	@25	@30	@5	@10	@15	@20	@25	@30
BinCorp	Gemini	✗	0.40 0.57	0.41 0.57	0.42 0.57	0.42 0.57	0.43 0.57	0.43 0.57	0.27 0.45	0.30 0.45	0.31 0.46	0.32 0.46	0.33 0.46	0.34 0.46
	SAFE	✗	0.54 0.77	0.57 0.78	0.58 0.78	0.59 0.78	0.60 0.78	0.61 0.78	0.42 0.69	0.48 0.71	0.51 0.71	0.53 0.71	0.55 0.72	0.57 0.72
	jTrans	✗	0.75 0.91	0.80 0.94	0.82 0.95	0.83 0.95	0.84 0.95	0.84 0.95	0.68 0.88	0.77 0.93	0.81 0.94	0.83 0.95	0.85 0.95	0.86 0.95
	CLAP	✗	0.87 0.91	0.89 0.94	0.90 0.94	0.91 0.94	0.91 0.94	0.91 0.94	0.83 0.88	0.87 0.92	0.89 0.94	0.90 0.94	0.91 0.94	0.91 0.95
	BinBERT	✗	0.74 0.88	0.78 0.90	0.79 0.90	0.80 0.91	0.80 0.91	0.81 0.91	0.66 0.84	0.73 0.87	0.76 0.88	0.78 0.88	0.79 0.88	0.80 0.89
	PalmTree	✗	0.59 0.76	0.61 0.76	0.62 0.77	0.63 0.77	0.63 0.77	0.64 0.77	0.48 0.68	0.52 0.69	0.54 0.69	0.56 0.70	0.57 0.70	0.58 0.70
	Trex	✗	0.61 0.81	0.65 0.82	0.66 0.82	0.67 0.82	0.67 0.82	0.68 0.82	0.50 0.74	0.56 0.76	0.60 0.76	0.62 0.77	0.63 0.77	0.65 0.77
MultiComp	Gemini	✗	0.61 0.84	0.49 0.71	0.46 0.67	0.46 0.66	0.47 0.66	0.48 0.66	0.25 0.39	0.31 0.51	0.34 0.54	0.36 0.55	0.38 0.56	0.40 0.56
	SAFE	✗	0.74 0.92	0.62 0.85	0.60 0.82	0.61 0.81	0.62 0.81	0.63 0.81	0.33 0.45	0.43 0.66	0.49 0.72	0.53 0.74	0.56 0.75	0.58 0.76
	jTrans	✗	0.74 0.90	0.63 0.80	0.60 0.77	0.60 0.76	0.61 0.76	0.61 0.76	0.32 0.43	0.43 0.59	0.48 0.65	0.50 0.67	0.53 0.68	0.54 0.69
	CLAP	✗	0.88 0.92	0.81 0.86	0.79 0.84	0.80 0.84	0.80 0.84	0.81 0.85	0.42 0.45	0.62 0.67	0.70 0.76	0.74 0.80	0.77 0.82	0.78 0.83
	BinBERT	✗	0.91 0.94	0.86 0.91	0.84 0.90	0.84 0.90	0.85 0.90	0.86 0.91	0.45 0.47	0.67 0.72	0.76 0.82	0.80 0.87	0.83 0.88	0.84 0.89
	PalmTree	✗	0.78 0.92	0.65 0.84	0.63 0.81	0.64 0.81	0.65 0.81	0.65 0.81	0.34 0.45	0.45 0.65	0.51 0.72	0.54 0.74	0.57 0.75	0.59 0.75
	Trex	✗	0.84 0.93	0.75 0.87	0.73 0.85	0.73 0.84	0.74 0.85	0.75 0.85	0.40 0.46	0.56 0.68	0.63 0.76	0.67 0.79	0.69 0.80	0.71 0.81

Research Questions

- RQ1.** What are the performance of ReSIM across various compilation toolchains?
- RQ2.** How is performance affected by the window on which ReSIM operates?
- RQ3.** When does ensembling with ReSIM provide performance gains?
- RQ4.** Is there a transfer of knowledge from the pre-training of ReSIM?

Our experimental evaluation was conducted on two hardware platforms. The first (S-A6000) is configured with four A600 GPUs, an AMD Ryzen Threadripper PRO 7985WX (64 cores), and Ubuntu 24.04.2 LTS. The second (S-A100) is an NVIDIA DGX A100 system with eight A100 GPUs, an AMD EPYC 7742 (64 cores), and Ubuntu 22.04.5 LTS.

We evaluate the performance on the function search task using the Recall and nDCG described in Section 2.1.

5.1 RQ1: Testing Across Toolchains

We evaluate ReSIM on seven embedding models (i.e., Gemini, SAFE, jTrans, CLAP, BinBERT, PalmTree, and Trex), considering the BinCorp and MultiComp datasets described in Section 4. The rationale for employing multiple datasets is to assess the effectiveness of ReSIM while mitigating potential biases that could arise from evaluating on a limited set of compilers or binaries: differently from the BinCorp dataset, whose binaries are compiled using the same toolchain as the fine-tuning corpus, MultiComp contains binaries produced by toolchains that are not used in the fine-tuning

dataset.

Table 1 presents the nDCG and Recall scores for all embedding models with and without DEEP re-ranking, evaluated at $k \in \{5, 10, 15, 20, 25, 30\}$ across both datasets using a window size of $w = 200$. To provide a clearer overview of the benefits introduced by our re-ranker, Table 2 reports the corresponding percentage improvements for $k \in \{5, 10, 20, 30\}$.

As shown in Table 2, the degree of improvement varies considerably across BFS models and datasets. The most substantial gains are observed for older embedding models, namely Gemini and SAFE. On BinCorp, Gemini achieves average nDCG gains of 37.4% and Recall improvements of 48.9%, while SAFE shows nDCG gains of 34.9% and Recall improvements of 43.1%. Similar trends emerge on MultiComp, with Gemini improving by 40.9% in nDCG and 53.3% in Recall, and SAFE by 30.7% in nDCG and 40.1% in Recall.

Modern transformer-based models still show significant improvements, typically in the 4–35% range on both metrics.

Specifically, on BinCorp, Trex benefits the most from re-ranking, with average gains of 25.5% in nDCG and 31.6% in Recall. On MultiComp, PalmTree shows the largest improvement, with average increases of 25.1% in nDCG and 35.2% in Recall. Overall, these results indicate that DEEP consistently improves performance across different embedding models.

In the remainder of this section, we focus on the top three re-ranked models (CLAP, jTrans, and BinBERT).

Table 2: Improvement (%) in nDCG and Recall at @5, @10, @20, and @30 after applying DEEP as reranker.

Dataset	BFS Model	nDCG				Recall				
		@5	@10	@20	@30	AVG	@5	@10	@20	AVG
BinCorp	Gemini	+42.5%	+39.0%	+35.7%	+32.6%	+37.4%	+66.7%	+50.0%	+43.8%	+35.3%
	SAFE	+42.6%	+36.8%	+32.2%	+27.9%	+34.9%	+64.3%	+47.9%	+34.0%	+26.3%
	jTrans	+21.3%	+17.5%	+14.5%	+13.1%	+16.6%	+29.4%	+20.8%	+14.5%	+10.5%
	CLAP	+4.6%	+5.6%	+3.3%	+3.3%	+4.2%	+6.0%	+5.7%	+4.4%	+4.4%
	BinBERT	+18.9%	+15.4%	+13.7%	+12.3%	+15.1%	+27.3%	+19.2%	+12.8%	+11.2%
	PalmTree	+28.8%	+24.6%	+22.2%	+20.3%	+24.0%	+41.7%	+32.7%	+25.0%	+20.7%
	Trex	+32.8%	+26.2%	+22.4%	+20.6%	+25.5%	+48.0%	+35.7%	+24.2%	+18.5%
MultiComp	AVG	+27.4%	+23.6%	+20.6%	+18.6%	+22.5%	+40.5%	+30.3%	+22.7%	+18.1%
	Gemini	+37.7%	+44.9%	+43.5%	+37.5%	+40.9%	+56.0%	+64.5%	+52.8%	+40.0%
	SAFE	+24.3%	+37.1%	+32.8%	+28.6%	+30.7%	+36.4%	+53.5%	+39.6%	+31.0%
	jTrans	+21.6%	+27.0%	+26.7%	+24.6%	+25.0%	+34.4%	+37.2%	+34.0%	+27.8%
	CLAP	+4.5%	+6.2%	+5.0%	+4.9%	+5.2%	+7.1%	+8.1%	+8.1%	+6.4%
	BinBERT	+3.3%	+5.8%	+7.1%	+5.8%	+5.5%	+4.4%	+7.5%	+8.7%	+6.0%
	PalmTree	+17.9%	+29.2%	+28.6%	+24.6%	+25.1%	+32.4%	+44.4%	+37.0%	+27.1%
	Trex	+10.7%	+16.0%	+15.1%	+13.3%	+13.8%	+15.0%	+21.4%	+17.9%	+14.1%
	AVG	+17.2%	+23.7%	+22.7%	+19.9%	+20.9%	+26.5%	+33.8%	+28.3%	+21.8%
										+27.9%

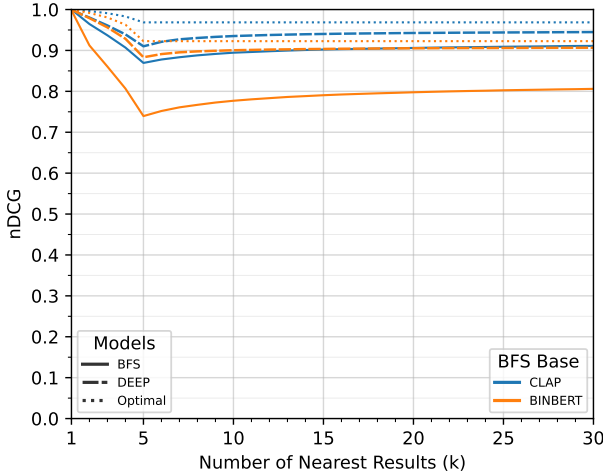


Figure 4: nDCG for CLAP and BinBERT with DEEP re-ranking ($w = 200$, $k \in [1, 30]$), evaluated on a pool of 25,000 functions and 5,000 queries from BinCorp.

5.1.1 Results on BinCorp.

Figures 4 and 5 show nDCG and Recall for CLAP and BinBERT on BinCorp: solid lines for baseline performance and dashed lines for DEEP. jTrans results are in Appendix A (Figures 14-15).

Without re-ranking, CLAP dominates across all k values for nDCG (0.87–0.91) and Recall (0.83–0.91), significantly outperforming BinBERT. After applying DEEP, as shown in Figures 4 and 5, the performance gap between CLAP and BinBERT substantially narrows, with both models achieving comparable results. From our experiments, jTrans + DEEP achieves comparable performance (0.94–0.95 nDCG) and slightly surpasses CLAP + DEEP in Recall by 0.01 points from $k \geq 10$. Although only jTrans and CLAP were trained on BinCorp functions (unlike BinBERT), DEEP brings all three models to similar performance levels.

5.1.2 Results on MultiComp.

Figures 6 and 7 show the results for CLAP and BinBERT on MultiComp. For completeness, results for jTrans are shown in Appendix A (Figures 16-17). We remark that DEEP has not been finetuned on binaries from MultiComp.

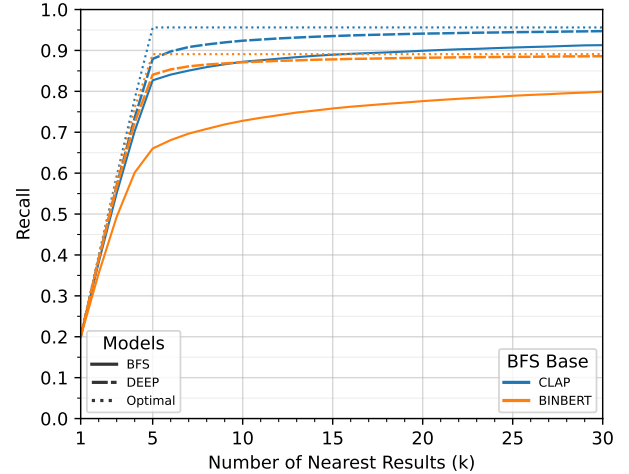


Figure 5: Recall for CLAP and BinBERT with DEEP re-ranking ($w = 200$ and $k \in [1, 30]$), evaluated on a pool of 25,000 functions and 5,000 queries from BinCorp.

Without re-ranking, BinBERT is the best performing model with average nDCG of 0.87 and Recall of 0.68, as expected given its fine-tuning on the same toolchains included in MultiComp. However, DEEP is still able to increase the performance, with BinBERT + DEEP being the best-performing model across all k values, with an average nDCG of 0.91 and Recall of 0.73. For CLAP and jTrans, DEEP improves the baseline average performance by 15.1% in nDCG and 20.4% in Recall. These results highlight DEEP’s strong generalization across unseen compilation toolchains.

5.1.3 Comparison with Optimal Performance

In the following, we examine how close DEEP approaches theoretical upper bound. In Figures 4 and 5 (for BinCorp) and Figures 6 and 7 (for MultiComp), we show with the dotted line the performance of the optimal re-ranker.

We can compute the optimal re-ranking for each query using the ground-truth labels in our datasets. Consider a query for which the pool P contains five semantically similar (i.e., relevant) functions. If the embedding-based retriever returns only four of these

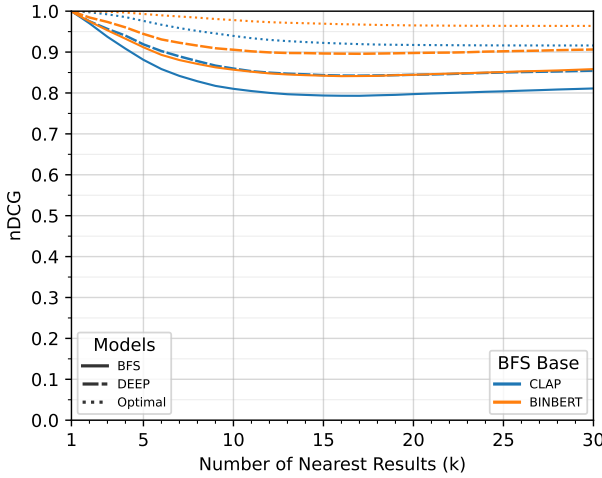


Figure 6: nDCG for CLAP and BinBERT with DEEP re-ranking (with $w = 200$, $k \in [1, 30]$), evaluated on a pool of 11,622 functions and 1,000 queries from MultiComp.

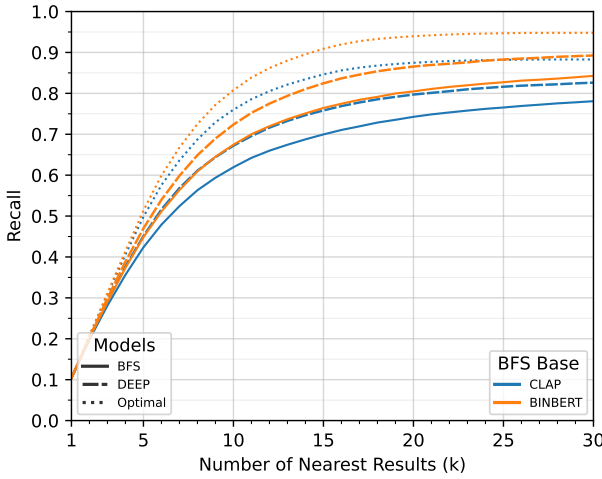


Figure 7: Recall for CLAP and BinBERT with DEEP re-ranking ($w = 200$ and $k \in [1, 30]$), evaluated on a pool of 11,622 functions and 1,000 queries from MultiComp.

five functions within the current candidate window, the optimal re-ranker would place all four retrieved relevant functions at the top of the ranking.

The gap between the embedding-based retrieval performance and the oracle upper bound indicates that, while bi-encoders identify most relevant functions within P , they do not rank them optimally. This gap quantifies the headroom available to re-ranking methods, and the gap between the upper bound and DEEP quantifies the goodness of our approach.

Consider jTrans on the BinCorp dataset: without re-ranking, it achieves average nDCG and Recall values of 0.83 and 0.76, respectively, falling short of the optimal 0.98 (nDCG) and 0.90 (Recall). DEEP improves performance to the near-optimal values of 0.95 for nDCG and 0.88 for Recall. For CLAP, the initial average performance stands at 0.91 (nDCG) and 0.83 (Recall), com-

pared to optimal values of 0.97 and 0.90. DEEP pushes performance to 0.94 for nDCG and 0.87 for Recall. Finally, on the MultiComp dataset, BinBERT achieves average nDCG and Recall values of 0.87 and 0.68, compared to optimal performance of 0.97 and 0.79. Notably, although DEEP’s fine-tuning dataset does not include the compilation toolchain used in MultiComp, it still improves performance to 0.91 in nDCG and 0.73 in Recall.

Answer to RQ1

On BinCorp, the re-ranker enhances performance across all models, yielding average gains of 22.5% in nDCG and 27.9% in Recall. The best-performing configuration is ReSIM with jTrans as the embedding model.

On MultiComp, our approach still yields substantial improvements of 20.9% in nDCG and 27.6% in Recall. Here, ReSIM with BinBERT as the underlying embedding model achieves the highest performance.

Overall, the performance gap between our DEEP and the optimal re-ranker is 3.8% for nDCG and 4.4% for Recall.

5.2 RQ2: Impact of the Window W

We now discuss the impact of the window size w on both the computational efficiency and the performance of ReSIM. As explained in Section 3, increasing or decreasing the value of w affects the time required to execute the re-ranker and may also influence Recall and nDCG. We restrict this analysis to the top three embedding models identified while answering RQ1: jTrans, CLAP, and BinBERT.

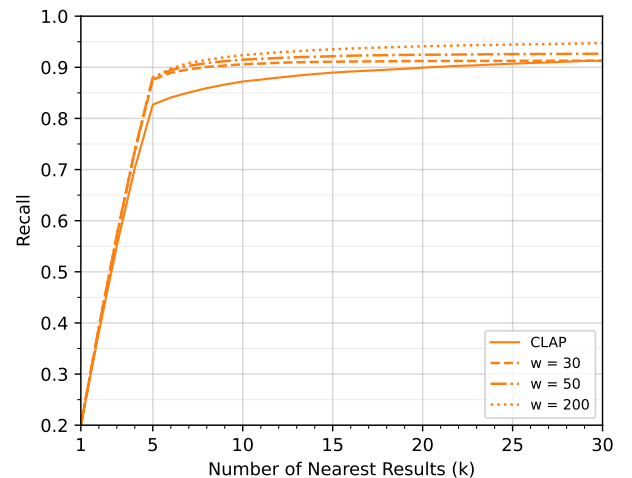


Figure 8: Recall for the CLAP model with DEEP re-ranking, ($w \in \{30, 50, 200\}$, $K \in [1, 30]$) evaluated on a pool of 25,000 functions and 5,000 queries from BinCorp.

5.2.1 Impact on nDCG and Recall

As expected, w acts as a parameter that influences the performance of the function search.

On BinCorp, the re-ranked CLAP achieves optimal overall performance at $w = 200$. The nDCG metric remains relatively stable across all window sizes for the considered values of k . In contrast, as visible in Figure 8, Recall exhibits more sensitivity to w : the performance is comparable across window sizes for $k \leq 10$, but diverges at higher k values, where larger windows provide clear advantages (e.g., while at $k = 5$ Recall coincides across all the values of w , at $k = 30$, Recall increases from 0.91 for $w = 30$ to 0.95 for $w = 200$). Similar patterns emerge for CLAP on MultiComp.

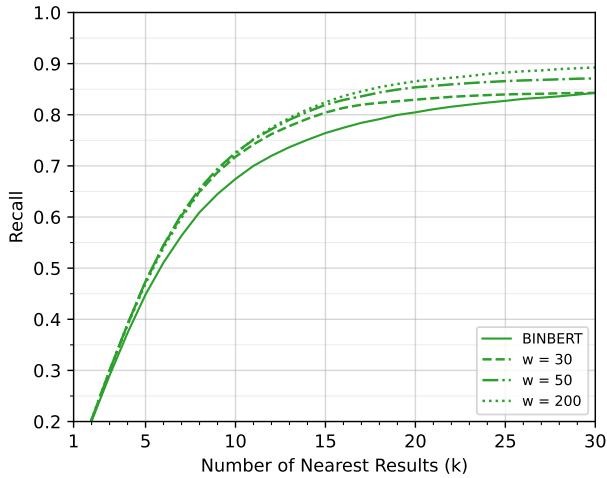


Figure 9: Recall for the BinBERT model with DEEP re-ranking ($w \in \{30, 100, 200\}$, $k \in [1, 30]$), evaluated on a pool of 11,622 functions and 1,000 queries from MultiComp.

The results for jTrans and BinBERT on BinCorp show that $w = 200$ yields the best performance for both models, with both metrics exhibiting greater sensitivity to window size compared to CLAP. On this dataset, both models show marked differences even at low k values, with average absolute differences at $k = 30$ of 0.06 for nDCG and 0.09 for Recall.

On MultiComp, the two models exhibit different behaviors. jTrans maintains the same performance gaps across all k values seen on BinCorp, whereas, as reported in Figure 9, BinBERT demonstrates minimal sensitivity for $k \leq 10$, with gaps emerging only as k increases.

Full results are reported in Table 4 (see Appendix B).

5.2.2 Impact on Computational Efficiency

Increasing the window size w increases the running time of the re-ranker module. Specifically, the total execution time for processing a query can be decomposed into three components: the time $t(\phi_i)$ for the embedding model ϕ_i to compute the embedding of the query function, the time $t(\text{sim})$ required to obtain the candidate window W based on embedding similarity, and

the time $t(\rho)$ required by the re-ranker to reorder the window W . While $t(\phi_i)$ and $t(\text{sim})$ are effectively independent of w , $t(\rho)$ scales with it.

In the following, we evaluate $t(\rho)$ when performing the re-ranking step for a single query on the S-A6000 hardware. We highlight that this value is independent of the specific embedding model ϕ_i , while it strictly depends on w . Indeed, $t(\rho)$ scales linearly with the window size w (e.g., halving w from 200 to 100 approximately halves the execution time; the same holds for $w = 50$ and $w = 30$). This observation is consistent with our theoretical analysis in Section 3. Specifically, $t(\rho)$ is equal to 16.5 seconds at $w = 30$, 27.6 seconds at $w = 50$, 54.9 seconds at $w = 100$, and 109.4 seconds at $w = 200$.

Both $t(\phi_i)$ and $t(\text{sim})$ are negligible compared to $t(\rho)$. Specifically, when considering the jTrans, CLAP, and BinBERT models, $t(\phi_i)$ exhibits an average of 0.013 seconds, while $t(\text{sim})$ is constant at 0.006 seconds. This is expected because sim is a vector–matrix multiplication, and the three models produce 768-dimensional embeddings. Therefore, the computational efficiency of ReSIM can be analyzed primarily as a function of w , while neglecting the other contributions. We stress that these times are for batch size; during $t(\text{sim})$, we compute the re-ranking score in parallel for all pairs that fit a batch size. The batch size depends on the architecture; in our test, we managed to use 50 as the batch size.

Answer to RQ2

The window size w significantly impacts ReSIM performance. Larger windows (e.g., $w = 200$) consistently yield better results for every value of $k \in \{1, 30\}$, with the performance gains exhibiting variability depending on the considered embedding model.

The re-ranking module dominates the per-query execution time, which increases approximately linearly with w . In contrast, the costs of embedding computation and similarity search are negligible. As a result, the end-to-end execution time is under one second without re-ranking, around 16 seconds at $w = 30$, and approximately 109 seconds at $w = 200$.

5.3 RQ3: Ensembling Models with ReSIM

In this section, we test the ensembling methodology. We ensemble the two best-performing re-ranked embedding models from Section 5.1. This is done as described in Section 3: we retrieve the top 100 results by applying ReSIM to jTrans and BinBERT, then order them by score and remove duplicates.

We evaluate this ensemble strategy on a dataset comprising functions from BinCorp and MultiComp. Specifically, starting from the pools described in Section 4.2, we select 1000 queries (500 from BinCorp and 500 from MultiComp), resulting in a final pool of 8,441

Table 3: nDCG and Recall for the considered BFS models with DEEP re-ranking ($w = 200$, $k \in \{5, 10, 15, 20, 25, 30\}$), evaluated on a pool of 8,441 functions jointly extracted from BinCorp and MultiComp. The **ENSEMBLE** row shows the performance obtained when ensembling the results of the two best-performing re-ranked models (i.e., jTrans and BinBERT).

BFS model	re-ranker	nDCG						Recall					
		@5	@10	@15	@20	@25	@30	@5	@10	@15	@20	@25	@30
jTrans	✗	0.82	0.79	0.78	0.78	0.79	0.80	0.58	0.68	0.72	0.75	0.76	0.78
	✓	0.93	0.90	0.89	0.89	0.89	0.89	0.68	0.80	0.84	0.86	0.86	0.87
BinBERT	✗	0.87	0.86	0.86	0.86	0.87	0.87	0.60	0.75	0.81	0.84	0.86	0.87
	✓	0.94	0.93	0.93	0.93	0.93	0.93	0.69	0.83	0.88	0.91	0.91	0.92
CLAP	✗	0.92	0.90	0.89	0.89	0.90	0.90	0.67	0.79	0.84	0.87	0.88	0.89
	✓	0.94	0.92	0.92	0.92	0.92	0.92	0.69	0.82	0.87	0.90	0.91	0.91
ENSEMBLE		0.94	0.94	0.94	0.94	0.94	0.95	0.69	0.85	0.90	0.93	0.94	0.95

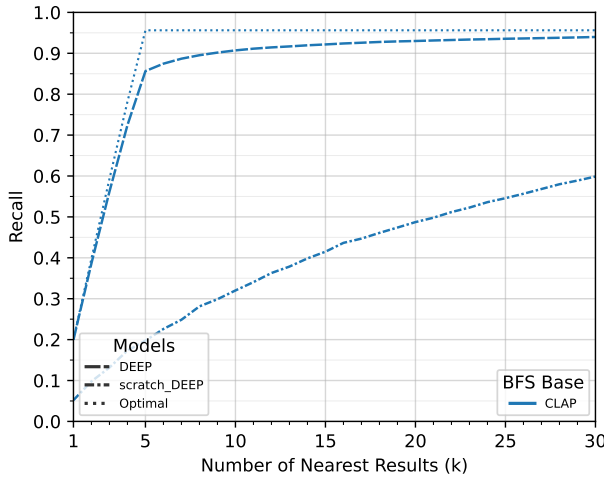


Figure 10: nDCG for the CLAP model with DEEP and scratch_DEEP re-ranking ($w = 200$, $K \in [1, 30]$), evaluated on a pool of 25,000 functions and 5,000 queries from BinCorp.

functions.

As expected, DEEP enhances the performance of the evaluated BFS models with respect to both nDCG and Recall. These improvements are further amplified through ensembling. Compared to the best individual re-ranked model on this pool (i.e., DEEP applied to CLAP), our aggregation yields an additional 2% increase in nDCG and 3% in Recall, with the gains being more pronounced for larger values of k ($k \geq 10$). The results are reported in Table 3. As we can see, the ensembling strategy outperforms both the non-re-ranked embedding models and the re-ranked ones. This arises from ensembling two embedding models, each of which exhibits state-of-the-art performance on a different toolchain.

Interestingly, the approach yields gains also on BinCorp (+1% in nDCG and +2% in Recall) and matches the DEEP re-ranked BinBERT on MultiComp. Details are in Appendix C.

Answer to RQ3

Ensembling embedding models yields a 3% Recall improvement on mixed datasets composed of multiple toolchains, outperforming any single embedding model. We believe this strategy is particularly effective on datasets built from toolchains that were not represented in the training data of an individual embedding model. On datasets composed of toolchains already seen during training, ensembling still improves or matches the performance of the non-ensembled re-ranking.

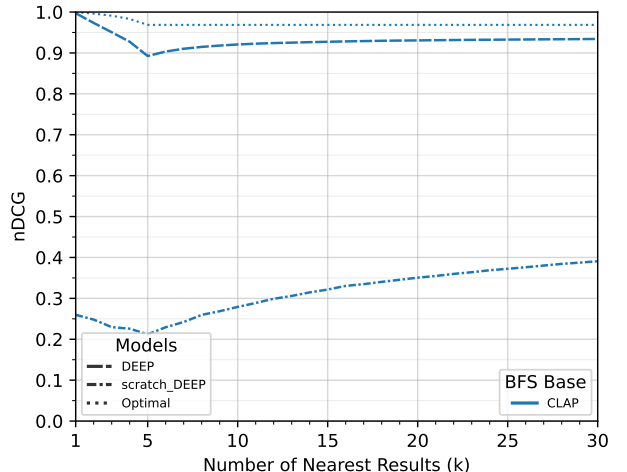


Figure 11: Recall for the CLAP model with DEEP and scratch_DEEP re-ranking, ($w = 200$, $K \in [1, 30]$), evaluated on a pool of 25,000 functions and 5,000 queries from BinCorp.

5.4 RQ4: Usefulness of Pre-Training

In this section, we investigate the impact of the transformer architecture and of the pre-training data on ReSIM. One may wonder whether the pre-training of DEEP is actually useful, as it is not specifically trained on assembly code and one could argue that most of the data it observes is not assembly. We show that this hypothesis is false: pre-training has a major impact on re-ranking performance.

To evaluate the impact of pre-training, we randomize 91.77% of the weights of DEEP (we randomize all

layers but the embedding and normalization one). This effectively obliterates all the knowledge stored in the model. We then fine-tune this “blank” model using the QLoRA methodology described in Section 3.1.3.

To avoid unnecessary energy consumption, we compare the performance of the blank model (scratch_DEEP) against the pre-trained one (DEEP) at the fifth training checkpoint. Ensuring that both models have seen the same data and training steps. A large performance gap at this early checkpoint is a strong indication that the pre-training data is indeed useful.

We evaluate random_DEEP and DEEP’s ability to re-rank CLAP results on the BinCorp pool from Section 4.2. The results in Figure 11 and Figure 10 clearly show pre-training’s significant benefit: at the fifth checkpoint, pre-trained DEEP on CLAP achieves an average of 0.92 nDCG and 0.93 Recall, whereas scratch_DEEP on CLAP achieves 0.14 in nDCG and 0.43 in Recall. We stress that QLoRA fine-tuning of DEEP updates only a small subset of parameters (namely, 0.57% of the total, which accounts for 43,655,168 parameters⁴), which further indicates that the pre-training knowledge acquired by DEEP is instrumental.

Answer to RQ4

Our experiments show a substantial transfer of information from the pre-trained DEEP. This may appear surprising, since its pre-training data is mostly natural language and high-level code. We speculate that this is because even non-domain-tailored pre-training improves the model’s reasoning capabilities.

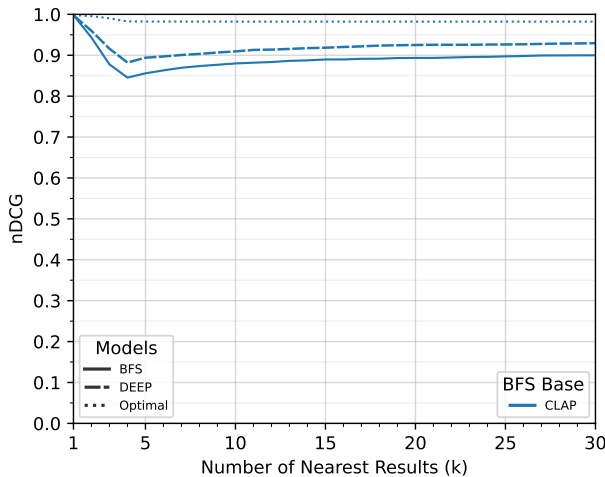


Figure 12: nDCG for the CLAP model with DEEP re-ranking ($w = 200$ and $k \in [1, 30]$), averaged across 70 CVEs.

⁴For comparison, a BERT transformer has roughly 110 million parameters

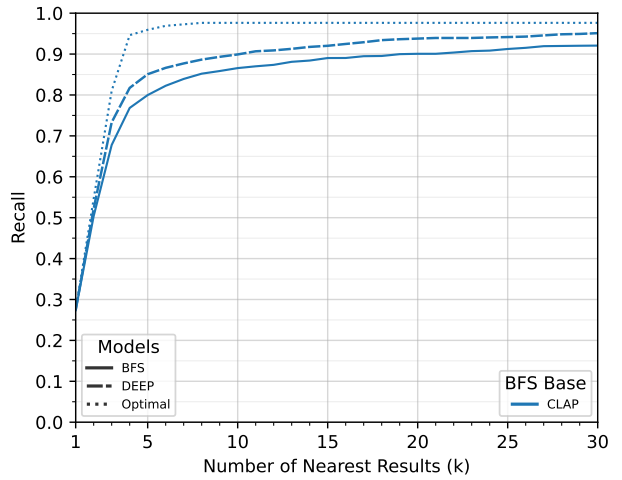


Figure 13: Recall for the CLAP model with DEEP re-ranking ($w = 200$ and $k \in [1, 30]$), averaged across 70 CVEs.

6 Vulnerability Detection

Following the approach of [52], we evaluate the capability of ReSIM of identifying vulnerable functions within packages affected by known CVEs. For this experiment, we consider CVEs extracted from the BinPool dataset [1]. This is a collection of real-world vulnerabilities extracted from different Debian packages and associated with specific CVEs, compiled for the x86-64 architecture using gcc with optimization levels ranging from O0 to O3. We follow the approach in Section 4.3 to disassemble the provided binaries; overall, our dataset comprises 138 CVEs affecting 64 distinct packages and 118 binaries across four Debian releases⁵, resulting in over 1.1 million functions.

We build an evaluation pool for each CVE, where each vulnerable function serves as a query against all functions from binaries affected by that CVE. We include only CVEs for which, after removing duplicates, we have at least 3 similar vulnerable functions. Figures 13 and 12 show the average Recall@ k and nDCG@ k across 70 CVE queries, with the dotted line indicating the performance of the optimal re-ranker.

The CLAP model achieves nDCG of 0.90 and Recall of 0.92 at $k = 1$. When enhanced with DEEP, both metrics improve to 0.93 and 0.95 respectively, yielding a relative gain of +3% for each metric and closing approximately half the gap to the optimal re-ranker. These improvements remain consistent across all k values: nDCG increases by +3.5%, while Recall shows a gain of +6.2% at $k = 5$, closing roughly one-third of the gap to the optimum for both metrics at this rank. Note that this gap decreases monotonically as k increases.

7 Related Works

This section surveys the main BFS systems and re-ranking strategies in IR, NLP, and source-code re-

⁵bookworm, bullseye, buster, and stretch

trieval.

7.1 Binary Function Similarity

Binary similarity research largely relies on embedding-based representations, where neural encoders map functions into dense semantic vectors. Apart from the embedding models used in this work, alternative approaches include **Asm2Vec** [8], **Zeek** [48], **CodeCMR** [60], and **InnerEye** [61], which capture features at the instruction level, represent code through intermediate program representations such as assembly or IR tokens, and encode local patterns of instruction sequences; **BinFinder** [46] and **Hermes-SIM** [15], which improve robustness to obfuscation and compiler optimizations; **CI-Detector** [20] and **OrderMatters** [59], which explicitly use control-flow and cross-function dependencies; **PROTST** [29] which uses a teacher-student approach where the transformer is trained on tasks of increasing difficulties.

While all previous systems adopt embedding-based strategies, others adopt different approaches. Specifically, **GMN** [24] is a GNN that implements a mechanism to match nodes across the CFGs of the functions to be analyzed; **Catalog1** [55] employs a fuzzy-hashing technique on raw bytes. Previous papers [2, 4, 30], have shown that these two models are inferior to some of the embedding models tested in our work. To the best of our knowledge, no existing function search system implements re-ranking.

7.2 Re-ranking

Re-ranking is a standard practice in information retrieval, aimed at refining an initial candidate set to improve ranking quality. Traditional learning-to-rank methods compute losses at the document, pair, or list level, while neural re-rankers extend this with representation-based (encode the query and candidate documents separately into embeddings), interaction-based (focus at the token or feature level interactions to capture rich contextual relationships), or hybrid architectures (combine both strategies to balance efficiency and fine-grained semantic understanding) [10, 14, 17, 34, 35, 49]. The advent of transformers [7] and benchmarks such as **MS MARCO** [36] initiated neural re-ranking at scale [25]. Cross-encoder architectures capture contextual interactions efficiently, as demonstrated by **monoBERT** and **duoBERT** [37, 39], while sequence-to-sequence models have been used for the generative-ranking paradigm estimating the likelihood of a certain query given a certain document [38, 40, 45]. Hybrid re-ranking systems combine several techniques in a complex pipeline, for example using non-neural ranking combined with a transformer-based ranking [11].

The most related application of re-ranking is the one to high level source-code retrieval, demonstrating that multi-stage retrieval generalizes beyond natural language. For instance, some approaches combine BM25 with a neural re-ranker, while others re-

fine fuzzy-matched candidates using sequential semantic similarity [9, 27]. These works show that applying a second-stage ranking is a recognized and effective practice, and our proposed method adheres to this established paradigm for binary function similarity. We want to highlight that both text and high-level source code represent application settings that are widely different from the binaries used in our paper.

8 Limitations

While our methodology presents significant advancements on the function search task and, broadly, on the binary function similarity problem, we identify certain limitations that could be addressed in future research.

In our evaluation, we did not focus on temporal efficiency; future studies may involve exploring lightweight re-ranker architectures and strategies.

A natural future direction is cross-architecture generalization. Our experiments indicate that the re-ranker generalizes across unseen x86-64 compiler toolchains; however, assessing its behavior on new architectures (e.g., ARM64, MIPS) remains an open question. To further evaluate the generalizability of our approach, future research may involve the creation of a larger benchmark, including a broader set of instruction sets, a greater number of open-source projects, and binaries specific to practical use-cases of these systems (i.e., malware detection/classification, copyright infringement).

9 Conclusions

In this paper, we presented ReSIM, a re-ranker-based pipeline to enhance the performance of embedding-based BFS detection systems when employed in the function search task.

We demonstrated across two distinct datasets that our re-ranker module, a decoder-only cross-encoder agnostic with respect to the underlying model, improves the ability of embedding-based BFS systems to retrieve, from large pools, functions compiled from the same source as a given query, in terms of nDCG and Recall. We have shown quantifiable improvements in several scenario, closing the gap towards an optimal system.

References

- [1] Sima Arasteh, Georgios Nikitopoulos, Wei-Cheng Wu, Nicolaas Weideman, Aaron Portnoy, Mukund Raghethaman, and Christophe Hauser. Binpool: A dataset of vulnerabilities for binary security analysis. In *Proceedings of the 33rd ACM International Conference on the Foundations of Software Engineering, FSE Companion 2025, Clarion Hotel Trondheim, Trondheim, Norway, June 23-28, 2025*, pages 1183–1187. ACM, 2025.
- [2] Fiorella Artuso, Marco Mormando, Giuseppe Antonio Di Luna, and Leonardo Querzoni. Binbert: Binary code understanding with a fine-tunable and

execution-aware transformer. *IEEE Transactions on Dependable and Secure Computing*, pages 1–18, 2024.

[3] Jane Bromley, Isabelle Guyon, Yann LeCun, Eduard Säckinger, and Roopak Shah. Signature Verification Using a Siamese Time Delay Neural Network. In *Proceedings of the 7th Annual Conference on Neural Information Processing Systems (NeurIPS '93)*, pages 737–744, 1993.

[4] Gianluca Capozzi, Daniele Cono D’Elia, Giuseppe Antonio Di Luna, and Leonardo Querzoni. Adversarial attacks against binary similarity systems. *IEEE Access*, 12:161247–161269, 2024.

[5] Gianluca Capozzi, Tong Tang, Jie Wan, Ziqi Yang, Daniele Cono D’Elia, Giuseppe Antonio Di Luna, Lorenzo Cavallaro, and Leonardo Querzoni. On the lack of robustness of binary function similarity systems. In *Proceedings of the 10th IEEE European Symposium on Security and Privacy (EuroS&P ’25)*, pages 980–1001, 2025.

[6] Hanjun Dai, Bo Dai, and Le Song. Discriminative Embeddings of Latent Variable Models for Structured Data. In *Proceedings of the 33rd International Conference on Machine Learning (ICML ’16)*, volume 48, pages 2702–2711, 2016.

[7] Jacob Devlin, Ming-Wei Chang, Kenton Lee, and Kristina Toutanova. BERT: pre-training of deep bidirectional transformers for language understanding. In *Proceedings of the Conference of the North American Chapter of the Association for Computational Linguistics: Human Language Technologies, (NAACL-HLT ’19)*, pages 4171–4186, 2019.

[8] Steven H.H. Ding, Benjamin C.M. Fung, and Philippe Charland. Asm2Vec: Boosting static representation robustness for binary clone search against code obfuscation and compiler optimization. In *Proceedings of the 40th IEEE Symposium on Security and Privacy (SP ’19)*, pages 472–489, 2019.

[9] Siddharth Gandhi, Luyu Gao, and Jamie Callan. Repository-level code search with neural retrieval methods. *arXiv preprint arXiv:2407.21783*, 2025.

[10] Debasis Ganguly, Dwaipayan Roy, Mandar Mitra, and Gareth J. F. Jones. Word embedding based generalized language model for information retrieval. In *Proceedings of the 38th International ACM SIGIR Conference on Research and Development in Information Retrieval (SIGIR ’15)*, pages 795–798, 2015.

[11] Luyu Gao, Zhuyun Dai, Zhen Fan, and Jamie Callan. Complementing lexical retrieval with semantic residual embedding. *arXiv preprint arXiv:1312.6199*, 2020.

[12] Aaron Grattafiori, Abhimanyu Dubey, Abhinav Jauhri, Abhinav Pandey, Abhishek Kadian, Ahmad Al-Dahle, Aiesha Letman, Akhil Mathur, Alan Schelten, Alex Vaughan, et al. The llama 3 herd of models. *arXiv preprint arXiv:2407.21783*, 2024.

[13] Daya Guo, Dejian Yang, Haowei Zhang, Junxiao Song, Ruoyu Zhang, Runxin Xu, Qihao Zhu, Shirong Ma, Peiyi Wang, Xiao Bi, et al. Deepseek-r1: Incentivizing reasoning capability in llms via reinforcement learning. *arXiv preprint arXiv:2501.12948*, 2025.

[14] Jiafeng Guo, Yixing Fan, Qingyao Ai, and W. Bruce Croft. A deep relevance matching model for ad-hoc retrieval. In *Proceedings of the 25th ACM International Conference on Information and Knowledge Management, CIKM 2016, Indianapolis, IN, USA, October 24–28, 2016*, pages 55–64, 2016.

[15] Haojie He, Xingwei Lin, Ziang Weng, Ruijie Zhao, Shuitao Gan, Libo Chen, Yue Ji, Jiashui Wang, and Zhi Xue. Code is not natural language: Unlock the power of semantics-oriented graph representation for binary code similarity detection. In *Proceedings of the 33rd USENIX Security Symposium (SEC ’24)*, 2024.

[16] Edward J. Hu, Yelong Shen, Phillip Wallis, Zeyuan Allen-Zhu, Yuanzhi Li, Shean Wang, and Weizhu Chen. Lora: Low-rank adaptation of large language models. *arXiv preprint arXiv:2106.09685*, 2022.

[17] Po-Sen Huang, Xiaodong He, Jianfeng Gao, Li Deng, Alex Acero, and Larry P. Heck. Learning deep structured semantic models for web search using clickthrough data. In *Proceedings of the 22nd ACM International Conference on Information and Knowledge Management (CIKM’13)*, pages 2333–2338, 2013.

[18] HuggingFace. Sentence Transformer: MPNet-Base-V2. <https://huggingface.co/sentence-transformers/all-mpnet-base-v2>, 2025.

[19] Kalervo Järvelin and Jaana Kekäläinen. Cumulated gain-based evaluation of IR techniques. *ACM Transactions on Information Systems (TOIS)*, 20(4):422–446, 2002.

[20] Ang Jia, Ming Fan, Xi Xu, Wuxia Jin, Haijun Wang, and Ting Liu. Cross-inlining binary function similarity detection. In *Proceedings of the 46th IEEE/ACM International Conference on Software Engineering (ICSE ’24)*, 2024.

[21] Vladimir Karpukhin, Barlas Oguz, Sewon Min, Patrick Lewis, Ledell Wu, Sergey Edunov, Danqi Chen, and Wen-tau Yih. Dense passage retrieval for open-domain question answering. In *Proceedings of the 25th Conference on Empirical Methods in Natural Language Processing (EMNLP ’20)*, 2020.

[22] Patrick Lewis, Ethan Perez, Aleksandra Piktus, Fabio Petroni, Vladimir Karpukhin, Naman Goyal, Heinrich Küttler, Mike Lewis, Wen-tau Yih, Tim Rocktäschel, et al. Retrieval-augmented generation for knowledge-intensive nlp tasks. *Advances in neural information processing systems*, 33:9459–9474, 2020.

[23] Xuezixiang Li, Yu Qu, and Heng Yin. Palmtree: Learning an assembly language model for instruction embedding. In *Proceedings of the 28th ACM SIGSAC Conference on Computer and Communications Security (CCS '21)*, page 3236–3251, 2021.

[24] Yujia Li, Chenjie Gu, Thomas Dullien, Oriol Vinyals, and Pushmeet Kohli. Graph matching networks for learning the similarity of graph structured objects. In *Proceedings of the 36th International Conference on Machine Learning (ICML '19)*, pages 3835–3845, 2019.

[25] Jimmy Lin, Rodrigo Nogueira, and Andrew Yates. Pretrained transformers for text ranking: BERT and beyond. *arXiv preprint arXiv:1312.6199*, 2020.

[26] Jimmy Lin, Rodrigo Nogueira, and Andrew Yates. *Pretrained transformers for text ranking: Bert and beyond*. Springer Nature, 2022.

[27] Chao Liu, Xin Xia, David Lo, Zhiwei Liu, Ahmed E. Hassan, and Shaping Li. Codematcher: Searching code based on sequential semantics of important query words. *ACM Trans. Softw. Eng. Methodol.*, 31:12:1–12:37, 2022.

[28] Yinhan Liu, Myle Ott, Naman Goyal, Jingfei Du, Mandar Joshi, Danqi Chen, Omer Levy, Mike Lewis, Luke Zettlemoyer, and Veselin Stoyanov. Roberta: A robustly optimized bert pretraining approach. *arXiv preprint arXiv:1907.11692*, 2019.

[29] Hanxiao Lu, Hongyu Cai, Yiming Liang, Antonio Bianchi, and Z. Berkay Celik. A progressive transformer for unifying binary code embedding and knowledge transfer. In *Proceedings of the 32nd International Conference on Software Analysis, Evolution and Reengineering (SANER '25)*, 2025.

[30] Andrea Marcelli, Mariano Graziano, Xabier Ugarte-Pedrero, Yanick Fratantonio, Mohamad Mansouri, and Davide Balzarotti. How Machine Learning Is Solving the Binary Function Similarity Problem. In *Proceedings of the 31st USENIX Security Symposium (SEC '22)*, pages 2099–2116, 2022.

[31] Luca Massarelli, Giuseppe Antonio Di Luna, Fabio Petroni, Leonardo Querzoni, and Roberto Baldoni. Investigating graph embedding neural networks with unsupervised features extraction for binary analysis. In *Proceedings of the 2nd Workshop on Binary Analysis Research (BAR)*, pages 1–11, 2019.

[32] Luca Massarelli, Giuseppe Antonio Di Luna, Fabio Petroni, Leonardo Querzoni, and Roberto Baldoni. Function Representations for Binary Similarity. *IEEE Transactions on Dependable and Secure Computing*, 19(4):2259–2273, 2022.

[33] Tomas Mikolov, Ilya Sutskever, Kai Chen, Greg S Corrado, and Jeff Dean. Distributed Representations of Words and Phrases and their Compositionality. In *Proceedings of the 27th Annual Conference on Neural Information Processing Systems (NeurIPS '13)*, pages 3111–3119, 2013.

[34] Bhaskar Mitra, Fernando Diaz, and Nick Craswell. Learning to match using local and distributed representations of text for web search. In *Proceedings of the 26th International Conference on World Wide Web, WWW 2017, Perth, Australia, April 3–7, 2017*, pages 1291–1299, 2017.

[35] Bhaskar Mitra, Eric T. Nalisnick, Nick Craswell, and Rich Caruana. A dual embedding space model for document ranking. *arXiv preprint arXiv:2407.21783*, 2016.

[36] Tri Nguyen, Mir Rosenberg, Xia Song, Jianfeng Gao, Saurabh Tiwary, Rangan Majumder, and Li Deng. MS MARCO: A human generated machine reading comprehension dataset. In *Proceedings of the Workshop on Cognitive Computation: Integrating neural and symbolic approaches 2016 co-located with the 30th Annual Conference on Neural Information Processing Systems (NIPS '16)*, 2016.

[37] Rodrigo Nogueira and Kyunghyun Cho. Passage re-ranking with BERT. *arXiv preprint arXiv:1312.6199*, abs/1901.04085, 2019.

[38] Rodrigo Nogueira, Zhiying Jiang, Ronak Pradeep, and Jimmy Lin. Document ranking with a pre-trained sequence-to-sequence model. In *Proceedings of the 58th Findings of the Association for Computational Linguistics (EMNLP '20)*, 2020.

[39] Rodrigo Nogueira, Wei Yang, Kyunghyun Cho, and Jimmy Lin. Multi-stage document ranking with BERT. *arXiv preprint arXiv:1312.6199*, 2019.

[40] Rodrigo Nogueira, Wei Yang, Jimmy Lin, and Kyunghyun Cho. Document expansion by query prediction. *arXiv preprint arXiv:1312.6199*, 2019.

[41] Aaron van den Oord, Yazhe Li, and Oriol Vinyals. Representation learning with contrastive predictive coding. *arXiv preprint arXiv:1807.03748*, 2018.

[42] Kexin Pei, Jonas Guan, Matthew Broughton, Zhongtian Chen, Songchen Yao, David Williams-King, Vikas Ummadisetty, Junfeng Yang, Baishakhi Ray, and Suman Jana. Stateformer: fine-grained type recovery from binaries using generative state modeling. In *Proceedings of the 29th ACM Joint European Software Engineering*

Conference and Symposium on the Foundations of Software Engineering (ESEC/FSE '21), pages 690–702, 2021.

[43] Kexin Pei, Zhou Xuan, Junfeng Yang, Suman Jana, and Baishakhi Ray. Learning approximate execution semantics from traces for binary function similarity. *IEEE Transactions on Software Engineering*, 49(4):2776–2790, 2023.

[44] Fabio Petroni, Samuel Broscheit, Aleksandra Piktus, Patrick Lewis, Gautier Izacard, Lucas Hosseini, Jane Dwivedi-Yu, Maria Lomeli, Timo Schick, Michele Bevilacqua, et al. Improving wikipedia verifiability with ai. *Nature Machine Intelligence*, 5(10):1142–1148, 2023.

[45] Ronak Pradeep, Rodrigo Nogueira, and Jimmy Lin. The expando-mono-duo design pattern for text ranking with pretrained sequence-to-sequence models. *arXiv preprint arXiv:1312.6199*, 2021.

[46] Abdullah Qasem, Mourad Debbabi, Bernard Lebel, and Marthe Kassouf. Binary function clone search in the presence of code obfuscation and optimization over multi-cpu architectures. In *Proceedings of the 2023 ACM Asia Conference on Computer and Communications Security (AsiaCCS '23)*, page 443–456, 2023.

[47] Nils Reimers and Iryna Gurevych. Sentence-bert: Sentence embeddings using siamese bert-networks. In *EMNLP*, 2019.

[48] Noam Shalev and Nimrod Partush. Binary similarity detection using machine learning. In *Proceedings of the 13th Workshop on Programming Languages and Analysis for Security*, pages 42–47, 2018.

[49] Yelong Shen, Xiaodong He, Jianfeng Gao, Li Deng, and Grégoire Mesnil. A latent semantic model with convolutional-pooling structure for information retrieval. In *Proceedings of the 23rd ACM International Conference on Conference on Information and Knowledge Management, CIKM 2014, Shanghai, China, November 3–7, 2014*, pages 101–110, 2014.

[50] Ashish Vaswani, Noam Shazeer, Niki Parmar, Jakob Uszkoreit, Llion Jones, Aidan N. Gomez, Łukasz Kaiser, and Illia Polosukhin. Attention is all you need. In *Proceedings of the 30th Annual Conference on Neural Information Processing Systems (NIPS '17)*, pages 5998–6008, 2017.

[51] Hao Wang, Zeyu Gao, Chao Zhang, Zihan Sha, Mingyang Sun, Yuchen Zhou, Wenyu Zhu, Wenju Sun, Han Qiu, and Xi Xiao. CLAP: learning transferable binary code representations with natural language supervision. In *Proceedings of the 33rd ACM SIGSOFT International Symposium on Software Testing and Analysis (ISSTA '24)*, pages 503–515. ACM, 2024.

[52] Hao Wang, Wenjie Qu, Gilad Katz, Wenyu Zhu, Zeyu Gao, Han Qiu, Jianwei Zhuge, and Chao Zhang. JTrans: Jump-aware transformer for binary code similarity detection. In *Proceedings of the 31st ACM SIGSOFT International Symposium on Software Testing and Analysis (ISSTA '22)*, pages 1–13, 2022.

[53] Lidan Wang, Jimmy Lin, and Donald Metzler. A cascade ranking model for efficient ranked retrieval. In *Proceedings of the 34th international ACM SIGIR conference on Research and development in Information Retrieval*, pages 105–114, 2011.

[54] Wai Kin Wong, Huaijin Wang, Zongjie Li, and Shuai Wang. Binaug: Enhancing binary similarity analysis with low-cost input repairing. In *Proceedings of the 46th IEEE/ACM International Conference on Software Engineering, ICSE 2024*, pages 7:1–7:13, 2024.

[55] xorpd. FCatalog. <https://www.xorpd.net/pages/fcatalog.html>.

[56] Xiaojun Xu, Chang Liu, Qian Feng, Heng Yin, Le Song, and Dawn Song. Neural network-based graph embedding for cross-platform binary code similarity detection. In *Proceedings of the 24th ACM SIGSAC Conference on Computer and Communications Security (CCS '17)*, pages 363–376, 2017.

[57] Yuhui Xu, Lingxi Xie, Xiaotao Gu, Xin Chen, Heng Chang, Hengheng Zhang, Zhengsu Chen, Xiaopeng Zhang, and Qi Tian. Qalora: Quantization-aware low-rank adaptation of large language models. *arXiv preprint arXiv:2309.14717*, 2023.

[58] An Yang, Anfeng Li, Baosong Yang, Beichen Zhang, Binyuan Hui, Bo Zheng, Bowen Yu, Chang Gao, Chengen Huang, Chenxu Lv, et al. Qwen3 technical report. *arXiv preprint arXiv:2505.09388*, 2025.

[59] Zeping Yu, Rui Cao, Qiyi Tang, Sen Nie, Junzhou Huang, and Shi Wu. Order matters: Semantic-aware neural networks for binary code similarity detection. In *Proceedings of the 34th AAAI Conference on Artificial Intelligence (AAAI '20)*, 2020.

[60] Zeping Yu, Wenxin Zheng, Jiaqi Wang, Qiyi Tang, Sen Nie, and Shi Wu. Codecmr: Cross-modal retrieval for function-level binary source code matching. In *Proceedings of the 34th Annual Conference on Neural Information Processing Systems (NeurIPS '20)*, 2020.

[61] Fei Zuo, Xiaopeng Li, Patrick Young, Lannan Luo, Qiang Zeng, and Zhexin Zhang. Neural machine translation inspired binary code similarity comparison beyond function pairs. In *Proceedings of the 26th Annual Network and Distributed System Security Symposium (NDSS '19)*, 2019.

A Impact on the Performance across Different Toolchains

In the following, we report the results when re-ranking the results of jTrans using our DEEP model. Figures 14 and 15 reports the nDCG and Recall over the BinCorp dataset, while Figures 16 and 17 reports the results over MultiComp.

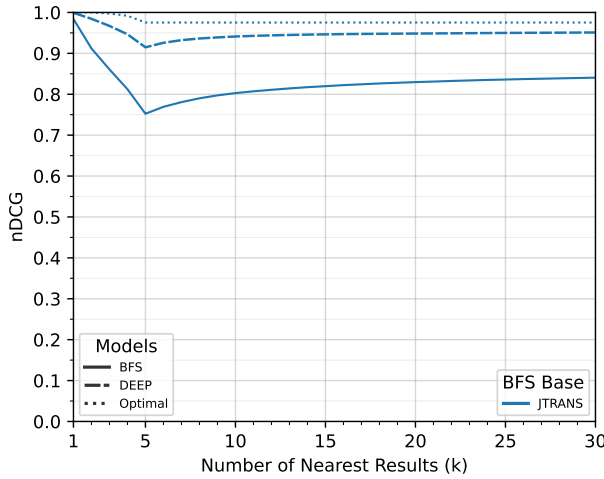


Figure 14: nDCG for the jTrans BFS model using DEEP as the re-ranker, with $w = 200$ and $K \in [1, 30]$, evaluated on a pool of 25,000 functions and 5,000 queries from BinCorp.

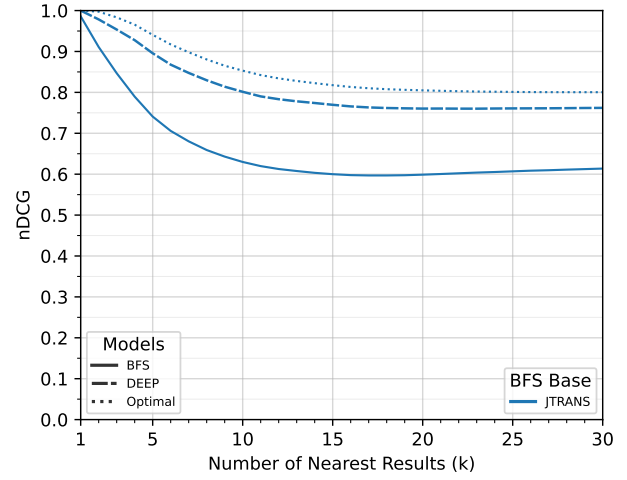


Figure 16: nDCG for the jTrans BFS model using DEEP as the re-ranker, with $w = 200$ and $K \in [1, 30]$, evaluated on a pool of 11,622 functions and 1,000 queries from MultiComp.

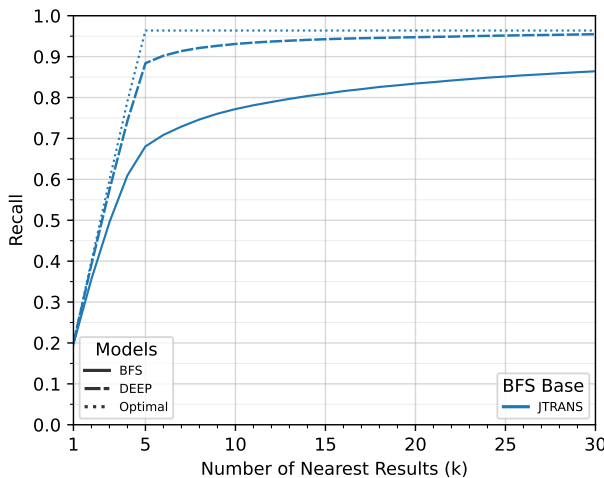


Figure 15: Recall for the jTrans BFS model using DEEP as the re-ranker, with $w = 200$ and $K \in [1, 30]$, evaluated on a pool of 25,000 functions and 5,000 queries from BinCorp.

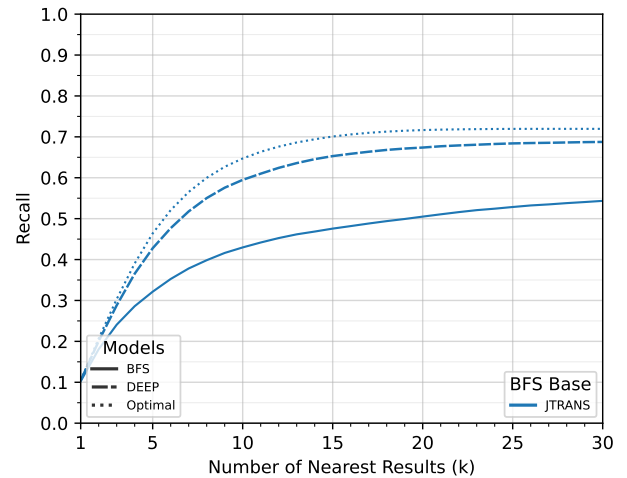


Figure 17: Recall for the jTrans BFS model using DEEP as the re-ranker, with $w = 200$ and $K \in [1, 30]$, evaluated on a pool of 11,622 functions and 1,000 queries from MultiComp.

B Impact of the Window Size

Table 4 shows the impact of the window size w on ReSIM.

Overall, $w = 200$ yields the best performance across all the models and pools. However, depending on the considered BFS model and the considered pool P , w differently influences the performance. Considering BinCorp, there increasing w constantly improves the performance when re-ranking results from jTrans and BinBERT. However, this is not the case of CLAP: for $k \leq 10$, the improvement is below 1% in average; thus, while reducing w may not affect the overall performance, this can produce a benefit from a computational point of view.

Moving to MultiComp, jTrans is the model that is mostly affected by the w parameter, with a monotonically increasing increment across the considered values of k ; contrarily, when considering CLAP and BinBERT with low values for k (i.e., $k \leq 10$), increasing w does not yield to a substantial improvement.

C Ensembling Performance on BinCorp and MultiComp

In the following, we analyze the impact of our ensembling strategy on pools extracted from BinCorp and MultiComp (see Table 5 for complete results). Details on these pools are provided in Section 4.2.

On BinCorp, our ensemble outperforms the strongest individual re-ranked model (DEEP on jTrans) by 1% in nDCG and 2% in Recall on average. On MultiComp, it matches the performance of re-ranked BinBERT across all k values, consistently ranking BinBERT’s top results at the highest positions.

Table 4: nDCG and Recall for the considered BFS models using DEEP as the re-ranker, with $w \in \{30, 50, 100, 200\}$ and $k \in \{5, 10, 15, 20, 25, 30\}$, evaluated on the BinCorp and MultiComp datasets.

Dataset	BFS model	Window size (w)	re-ranker	nDCG					Recall					
				@5	@10	@15	@20	@25	@30	@5	@10	@15	@20	
BinCorp	jTrans	—	✗	0.75	0.80	0.82	0.83	0.84	0.84	0.68	0.77	0.81	0.83	0.85
		30	✓	0.88	0.89	0.90	0.90	0.90	0.90	0.84	0.86	0.86	0.86	0.86
		50	✓	0.90	0.91	0.91	0.92	0.92	0.92	0.86	0.89	0.89	0.89	0.90
		100	✓	0.91	0.93	0.94	0.94	0.94	0.94	0.88	0.92	0.92	0.93	0.93
		200	✓	0.91	0.94	0.95	0.95	0.95	0.95	0.88	0.93	0.94	0.95	0.95
	CLAP	—	✗	0.87	0.89	0.90	0.91	0.91	0.91	0.83	0.87	0.89	0.90	0.91
		30	✓	0.91	0.93	0.93	0.93	0.93	0.93	0.88	0.91	0.91	0.91	0.91
		50	✓	0.91	0.93	0.93	0.94	0.94	0.94	0.88	0.91	0.92	0.92	0.93
		100	✓	0.91	0.93	0.94	0.94	0.94	0.94	0.88	0.92	0.93	0.93	0.94
		200	✓	0.91	0.94	0.94	0.94	0.94	0.94	0.88	0.92	0.94	0.94	0.95
MultiComp	jTrans	—	✗	0.74	0.78	0.79	0.80	0.80	0.81	0.66	0.73	0.76	0.78	0.79
		30	✓	0.84	0.85	0.85	0.85	0.85	0.85	0.78	0.80	0.80	0.80	0.80
		50	✓	0.86	0.74	0.70	0.69	0.68	0.68	0.40	0.53	0.56	0.58	0.58
		100	✓	0.88	0.77	0.74	0.73	0.72	0.73	0.41	0.56	0.61	0.63	0.64
		200	✓	0.90	0.80	0.77	0.76	0.76	0.76	0.43	0.59	0.65	0.67	0.69
	CLAP	—	✗	0.88	0.81	0.79	0.80	0.80	0.81	0.42	0.62	0.70	0.74	0.77
		30	✓	0.92	0.85	0.83	0.82	0.83	0.83	0.45	0.66	0.73	0.76	0.78
		50	✓	0.92	0.86	0.84	0.84	0.84	0.84	0.45	0.67	0.75	0.78	0.80
		100	✓	0.92	0.86	0.84	0.84	0.85	0.85	0.45	0.67	0.76	0.79	0.81
		200	✓	0.92	0.86	0.84	0.84	0.85	0.85	0.45	0.67	0.76	0.80	0.82
MultiComp	BinBERT	—	✗	0.91	0.86	0.84	0.84	0.85	0.86	0.45	0.67	0.76	0.80	0.84
		30	✓	0.95	0.90	0.88	0.88	0.88	0.88	0.47	0.72	0.80	0.83	0.84
		50	✓	0.95	0.91	0.89	0.89	0.89	0.89	0.47	0.73	0.82	0.85	0.87
		100	✓	0.95	0.91	0.90	0.90	0.90	0.91	0.47	0.73	0.82	0.86	0.88
		200	✓	0.94	0.91	0.90	0.90	0.90	0.91	0.47	0.72	0.82	0.87	0.88

Table 5: nDCG and Recall scores when considering $w = 200$ and $k \in \{5, 10, 15, 20, 25, 30\}$, evaluated on a pool of 25,000 functions extracted from the BinCorp dataset. The **ENSEMBLE** row shows the performance obtained when ensembling the re-ranked results from jTrans and BinBERT.

Dataset	BFS model	re-ranker	nDCG					Recall						
			@5	@10	@15	@20	@25	@30	@5	@10	@15	@20	@25	
BinCorp	jTrans	✗	0.75	0.80	0.82	0.83	0.84	0.84	0.68	0.77	0.81	0.83	0.85	0.86
		✓	0.91	0.94	0.95	0.95	0.95	0.95	0.88	0.93	0.94	0.95	0.95	0.95
	CLAP	✗	0.87	0.89	0.90	0.91	0.91	0.91	0.83	0.87	0.89	0.90	0.91	0.91
		✓	0.91	0.94	0.94	0.94	0.94	0.94	0.88	0.92	0.94	0.94	0.94	0.95
	BinBERT	✗	0.74	0.78	0.79	0.80	0.80	0.81	0.66	0.73	0.76	0.78	0.79	0.80
		✓	0.88	0.90	0.90	0.91	0.91	0.91	0.84	0.87	0.88	0.88	0.88	0.89
	ENSEMBLE			0.92	0.95	0.95	0.96	0.96	0.96	0.89	0.94	0.95	0.96	0.97
	jTrans	✗	0.74	0.63	0.60	0.60	0.61	0.61	0.32	0.43	0.48	0.50	0.53	0.54
		✓	0.90	0.80	0.77	0.76	0.76	0.76	0.43	0.59	0.65	0.67	0.68	0.69
	CLAP	✗	0.88	0.81	0.79	0.80	0.80	0.81	0.42	0.62	0.70	0.74	0.77	0.78
		✓	0.92	0.86	0.84	0.84	0.84	0.84	0.45	0.66	0.73	0.76	0.78	0.80
	BinBERT	✗	0.91	0.86	0.84	0.84	0.85	0.86	0.45	0.67	0.76	0.80	0.83	0.84
		✓	0.94	0.91	0.90	0.90	0.90	0.91	0.47	0.72	0.82	0.87	0.88	0.89
MultiComp	ENSEMBLE													
	jTrans	✗	0.74	0.63	0.60	0.60	0.61	0.61	0.32	0.43	0.48	0.50	0.53	0.54
		✓	0.90	0.80	0.77	0.76	0.76	0.76	0.43	0.59	0.65	0.67	0.68	0.69
	CLAP	✗	0.88	0.81	0.79	0.80	0.80	0.81	0.42	0.62	0.70	0.74	0.77	0.78
		✓	0.92	0.86	0.84	0.84	0.85	0.85	0.45	0.67	0.76	0.80	0.82	0.83
	BinBERT	✗	0.91	0.86	0.84	0.84	0.85	0.86	0.45	0.67	0.76	0.80	0.83	0.84
		✓	0.94	0.91	0.90	0.90	0.90	0.91	0.47	0.72	0.82	0.87	0.88	0.89